Progress in Spectral-Spatial interferometry at multi-THz frequencies - Potential applications

Peter Ade,
Amber Hornsby,
Enzo Pascale,
Rashmi Sudiwala
School of Physics and Astronomy
Cardiff Unviersity, Cardiff
Wales, UK

Roser Juanola-Parramon,
Nicola Baccichet,
*Giorgio Savini**
Optical Science Laboraotory
Dept. of Physics and Astronomy
University College London
London, UK
* Corresponding author. Email: g.savini@ucl.ac.uk

Colm Bracken,
Anthony Donohoe,
Anthony Murphy,
Credihe O'Sullivan
National University of Ireland Maynooth
Maynooth, Dublin
Telephone: (800) 555–1212
Fax: (888) 555–1212

Abstract—**Spectral-spatial interferometry pioneered in a narrow band in the near infrared has not enjoyed much exploitation as a technique. Proposed as a promising modulation method for a potential Far-infrared future satellite, a period of study was performed on two testbeds to improve and evolve this technique in the laboratory in order to simplify some of the technical aspects and the data analysis involved. Here we will present an update on the successful upgrade of a previous wideband millimetric (0.3-1.0 THz) testbed to a far-IR (11-14THz) one, as well as the ongoing progress on a broadband setup for an imaging system with a commercial thermal- or mid-IR (8 to 12 micron or 25-35 THz) camera currently working as imaging FTS. Source size, coherence and technical issues are discussed.**

I. INTRODUCTION

The first multi-Fourier transform experiments performed by Mariotti and Ridgeway (MR88)[1] and Itoh and Ohtsuka in similar fashion gave a glimpse of the possibilities that Double-Fourier modulation (or spatial-spectral interferometry) allow. MR88 focused on the application of this technique to astronomy following in the pioneering footsteps of Michelson, thus fuelling the interest in developing further concepts at different wavelengths to improve angular resolution measurements while preserving wide band spectrophotometry.

The spectral spatial interferometry potential was immediately captured in the suggestion that this technique could be the one of choice for the first Far-infrared interferometer in space (SPIRIT [2] and FIRI-ESACDF [3]). NASA [4] invested in an optical scaled version of what the SPIRIT concept would produce in order to reproduce the original experiment in a fashion that would demonstrate intuitively through a simple scaling the vast potential of this concept.

With the intention to reproduce the Mariotti and Ridgeway experiment at longer wavelengths and to demonstrate and extend the feasibility of this technique to other frequency ranges and broader frequency bands (and more importantly at those frequencies which matter for the technology in question), a first testbed in the Far Infrared (300GHz-1THz) was assembled in a coordinated effort at Rutherford Appleton Laboratories. Subsequently with the involvement of Cardiff University and University College London, the testbed obtained its first double

modulation and spectral-spatial fringes in a laboratory environment [5].

Finally, in order to study other effects such as off-axis corrections, imaging algorithms as well as the effect of the thermal emission of the environment (critical for a space-based mission) a third testbed was designed [6]. In the latter (still in development phase) we aimed to study how variations in the operational temperature of the optics affect the data acquisition and the analysis as well as the added complexities of an imaging system. To do this we elected to work in the wavelength range where the peak of environment thermal emission occurs and where large format detectors are relatively "cheap" when compared to the sub-mm counterparts. The latter testbed is in construction and has so far tested the phase delay stage and detecting camera by working as an imaging Fourier spectrometer while awaiting the final installation of a large collimator to allow the re-assembly of the fore-optics to resemble those of a spatial interferometer.

In the following section we will give a short description of the latest work performed on both testbeds and how they operate highlighting recent improvements while referring to more details in previous respective works [5],[6].

Fig. 1. The Cardiff Far-infrared spectral-spatial testbed extends over 8m of optical path (mostly collimated). The collimator is a 1m spherical segment and the two telescopes are two pairs of off-axis parabolic mirrors which compress the beam from the ∼ 7.5cm wide aperture to the 2.5 cm beam travelling on the optical bench.

II. THE FAR-IR CRYOGENIC TESTBED

The basic layout of the Far-IR testbed originally assembled with a wide-band mm-wave beam-combiner working from

$300\mu m$ to 3mm can be seen in fig.1 of [5] and can be seen re-arranged in the basic same configuration in Fig.1 of this paper. The wide-band mm-wave beam combiner and cryostat optics have been replaced to work at much shorter wavelength in the 21-27 μm atmospheric band. This band is well represented by the maximum envelope of all the spectra plotted in Fig.2.

Atmospheric lines in the same Fig.2 can be seen "invading" the band of interest. These lines are useful in this measurement as they serve as a consistency test between spectral measurements and as effective calibrators.
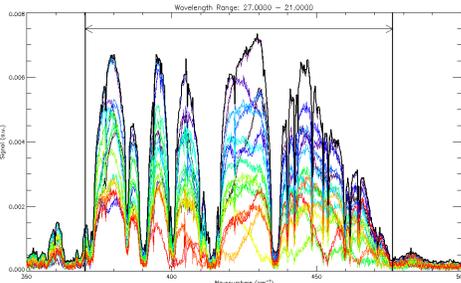
Fig. 2. The spatial modulation of the overall spectral source (thick black envelope) can be seen as the two-telescope baseline increases. The coloured modulated spectra (from violet, to blue, green, yellow, red show the same spectra modulated by the spatial interference as the two telescopes are moved apart. The atmospheric telluric lines are well apparent in the 20-25 micron range (12-15 THz).

In the Double-Fourier set-up, two small co-aligned telescopes receive the incoming collimated beam from a common source scene at the focus of the collimator (in this case a 1m segment of a spherical mirror). The source and collimator act as a sky simulator transforming spatial structure at the collimator's focal plane into angles of arrival at the telescopes which depend on a combination of focal plane scale of the collimator and the angle which its optical axis forms with the telescope axes. The latter will dictate the portion of spatial fringe sampled by the system as the baseline between telescopes varies.

The inputs from the two telescopes are combined after one of them is phase delayed as in the case of a classical Fourier transform spectrometer. The resulting FT sets of data (for each baseline length) is shown in different colours in Fig.2. The spectra is effectively modulated by the spatial interference induced by the combination of telescope separation and angle of arrival of the source. This modulation is faster as the sources separate. If the observer were viewing a mono-chromatic source, he would observe the corresponding delta-function oscillating in amplitude to reflect the spatial interference pattern as the baseline separates.

This reflects the way in which one can crudely analyse the data, by considering spectral bins where sufficient signal is present and plotting the integrated signal vs cycles (baseline/λ) and doing this for each wavelength will produce the set of points in Fig.3. These were then overlaid with a first approximate best fit FT of the spatial structure generating the spectral-spatial modulation observed as the thick black line. The nature of the approximation lies in the symmetry of the slit-source which was fourier transformed. In reality more care and complexity could have been considered in using an-asymmetrical source. Such an asymmetry (known to the

users) is present slightly both in size, but it is also apparent in amplitude since the fast spatial modulation generated by the two slits does not cancel down to zero implying a slight unbalance of the two sources.
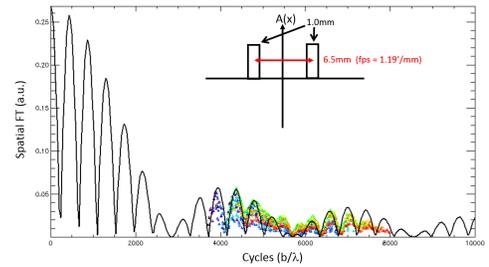
Fig. 3. Cosine transform of each spectral bin is performed and plotted vs (baseline/wavelength). The different colours represent the varying wavelength bin used. The black thin line, a preliminary analysis best fit of all the combined cosine transforms and corresponds to the Fourier Transform of a double slit source both measuring 1mm in width and positioned at 6.5mm from each other (inset sketch).

Further progress will be sought by adopting a 3 slit source on a rotating mount in order to simulate a 2D interferometer and test other reconstruction issues which could be ignored given the one dimensional nature of the baselines.

III. THE MID-IR IMAGING TESTBED

In the previous section the testbed described can be modified accordingly and through the substitution of a few optical elements (beam-combiner and filters) to work in a number of different ranges spanning from 3mm up to 20 μm. Whilst the technology required for this experiment relies on substantial and complex technology heritage, one major advantage is retained which is the fact that a single pixel is employed with a substantial collecting area at the focus of the system (a smooth walled conical horn in this specific case). Furthermore given the long wavelength, we are generally in the Rayleigh-Jeans portion of the spectrum and temperature variations of the environment and the optics have little to no impact on the final measurements.
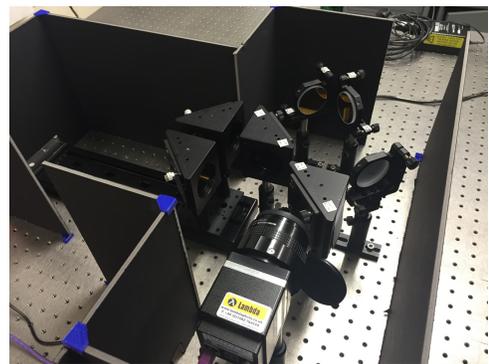
Fig. 4. The thermal-IR testbed setup initially assembled as an imaging FTS to verify the alignment and performance of the translation stage.

For this reason the UCL testbed was initially set up: the addition of imaging capability as well as the spectral range shift to a region most sensitive to the peak thermal emission of the optics used. Lessons learned in this testbed

will prove valuable in future studies on space-based instrument requirements.

To verify the basic functionality of the testbed elements (detector camera and moving stage) the testbed was initially set up and aligned in an FTS configuration (Fig.4) where the FTS stage can be seen on the left and the source is at the far top right corner of the picture.
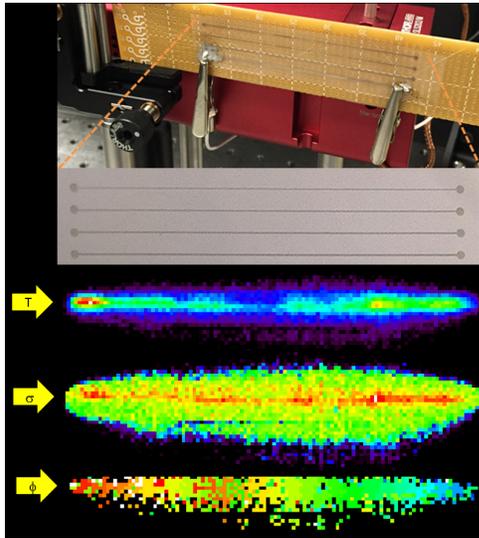
Fig. 5. Top: Setup of the weak thermal source (a heated printed electronics circuit line) which acted as spatial structure for the thermal IR camera. Below the picture of the electronic print is the Temperature data in rainbow colour (25-45°C), below that the standard deviation of the timeline acquired as a function of the optical delay stage (used as a proxy for the identification of fringe visibility (arbitrary units), and at the bottom, the position of the ZPD as a function of time for each of the pixels of the image. With the ZPD first appearing at the far right of the image and travelling to the left end of the strip.

The source used was a weak spatial thermal source obtained via Joule heating a single printed electronic strip (on a polypropylene substrate),to a maximum of 45 degrees Celsius. As the FTS was scanned the max recorded value was registered as shown below the strip picture in Fig.5. A proxy of fringe visibility for the spectrometer was taken by looking at the standard deviation of the interferogram (after noting that the average S/N ratio of the biggest IG signals was ∼30). Additionally, the position of the ZPD for each scan was noted and colour coded to verify how the ZPD would temporally move across the image (typical of the case where the image plane of the scene presented is not exactly orthogonal to the optical axis of the spectrometer).

By placing a temperature threshold on the thermal image the hottest (35-45°C) and warm (25-35°C) pixels were identified, Fourier transformed and co-added to create to spectra which were then normalized and compared. A non-negligible shift in the peak of this recovered thermal emission spectra can be observed in Fig.6 and is expected. No attempt to fit an actual black-body curve was performed due to the added complexity of the camera spectral sensitivity as well as the lens transmission in addition to this being beyond the scope of this test. The IR testbed has now been re-assembled to employ a single beam-combiner and two parallel output ports which will impact on the lower portion of a large (81 cm) diameter
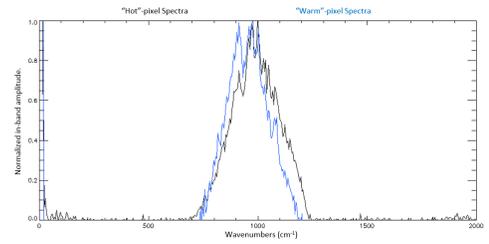
Fig. 6. Crude average FT of the pixels lying in one line coincident with the printed electronic strip (black) compared to the normalized average FT of all the interferograms of the pixels where a ZPD was detected above a threshold of 5σ of the noise level of the IG acquired. A small but obvious shift can be noted between the two thermal emission envelopes. No black-body fit has been attempted due to the complex convolution of the camera specific sensitivity as well as the camera lens specific transmission.

spherical collimator to be mounted at the edge of the optical bench.
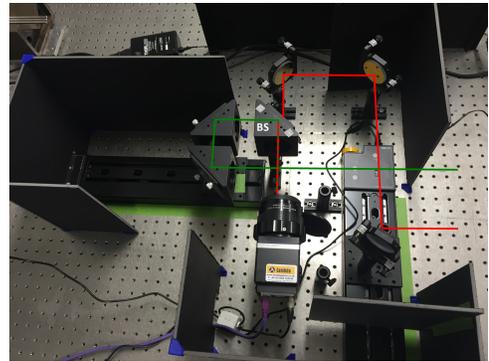
Fig. 7. The same testbed shown in Fig.4 is now modified to have two outgoing beams which join at the beam combiner from two adjacent optical ports. The collimator will be installed at the far end of the optical bench with a folded path (given its size) maintained on a plane above the testbed.

IV. DISCUSSION

We have shown ongoing progress in the development of the Cardiff Far-Infrared testbed which demonstrates further the capability of adapting to a particular wavelength range of operation while maintaining the main opto-mechanical features. There remain substantial complexities in the alignment of both systems where qualitative measurements can be performed trivially but which for precise quantitative analysis additional metrology on most of their optical components is required. It is also worth mentioning that the sources in question play a significant role in the demonstration of such systems. The Far-infrared system relies on a bright Hg-arc lamp viewed through machined slits of a size which given the magnification of the system is tailored to view a few spatial fringes. The imaging camera testbed on the other hand requires careful planning of the source which if not magnified (as is the plan with the collimator) and will require image-matching at pixel level to preserve coherency which can be quite challenging given the few-micron size of its pixels.

As is the case for classical interferometers, knowledge of what is the desired physical scale to which the instrument should be sensitive will help the user in designing the range of baselines available. This reduces the practicality and uses of

such a system compared to a direct imaging or a spectral system, but should be considered for more specific, high-angular resolution applications, albeit possibly remaining confined to either space applications due to the absence of atmospheric-induced coherence issues or near-field applications.

REFERENCES

[1] J.M. Mariotti and S. T. Ridgway, *Double Fourier spatio-spectral interferometry - combining high spectral and high spatial resolution in the near infrared*, A&A, **195**, pp.350-363 (1988).

[2] D.T. Leisawitz et al., *The Space Infrared Interferometric Telescope (SPIRIT): High-resolution imaging and spectroscopy in the far-infrared*, Adv. Sp. Res., **40**, pp.689 (2007).

[3] A. Lyngvi et al., *Far Infra-Red Interferometer (FIRI): Technology reference study*, ESA CDF Study Report, IAC-06-A3.1.05 (2006).

[4] D.T. Leisawitz et al., *Wide-field imaging interferometry testbed I: purpose, testbed design, data and synthesis algorithms*, in *Interferometry in space*, M.Shao ed., Proc. SPIE, **4852** A&A, **195**, pp.255 (2003).

[5] W.F. Grainger et al., *A Demonstration of Spectral and Spatial Interferometry at THz Frequencies*, in *App.Opt.*, **51**, **12**, pp.2202-2211 (2012).

[6] D.T. Leisawitz et al., *Wide-field imaging interferometry testbed I: purpose, testbed design, data and synthesis algorithms*, in *Interferometry in space*, M.Shao ed., Proc. SPIE, **4852** A&A, **195**, pp.255 (2003).